

# Longitudinal stacking of ion beams with pulsed electron beam cooling

He Zhao<sup>1</sup> and Lijun Mao<sup>1\*</sup>*Institute of Modern Physics, Chinese Academy of Sciences, Lanzhou 730000, China* (Received 27 July 2022; accepted 16 February 2023; published 7 March 2023)

Longitudinal ion beam stacking with the combination of barrier rf system and beam cooling has been demonstrated in several experiments. Based on the bunching effect found in the pulsed electron beam cooling experiment at HIRFL-CSRm, we propose a new beam stacking scheme using only pulsed electron beam, in which the barrier voltage and cooling effect can be realized simultaneously. In this paper, we introduce this longitudinal stacking scheme along with the theory of beam dynamics and present a simple analytical model. The simulation demonstrates that this approach could be a useful beam stacking technique without the need for barrier bucket hardware. Moreover, the optimization and limitation of this stacking scheme are discussed, and the effect of the electron beam distribution on the barrier voltage is studied. We expect this stacking method can be applied to accumulate RIBs in low and medium energy storage rings for high-precision experiments, such as the SRing of the HIAF project.

DOI: [10.1103/PhysRevAccelBeams.26.030101](https://doi.org/10.1103/PhysRevAccelBeams.26.030101)

## I. INTRODUCTION

Since it was first proposed in 1983 by Griffin [1], the barrier bucket method has become an important tool in a variety of beam manipulation applications, such as momentum mining, beam compression, and beam stacking [2]. With the surge in worldwide interest in the beam intensity frontier, high intensity beam stacking in synchrotrons becomes an important topic. As one of the developed longitudinal beam stacking methods, the barrier bucket scheme has been successfully applied to several synchrotrons. In the 1980s, the first attempt is made to use the barrier rf system as a gap preservation for antiproton stacking in the Fermilab Accumulator ring. Since then, beam manipulation using a barrier bucket system has been widely used and studied in a number of synchrotrons at Fermilab, BNL, KEK, and CERN [3–6].

Recently, the interest in the barrier rf system was stimulated in heavy-ion storage rings due to the development of beam cooling methods. A barrier bucket scheme associated with beam cooling could be an effective method for longitudinal beam stacking in synchrotrons. In 2007, longitudinal beam stacking of the bare  $^{40}\text{Ar}^{18+}$  ions at 65.3 MeV/u using a barrier bucket and continuous electron cooling was tested in the experimental storage ring (ESR) at

GSI [7]. Later, the stacking of 400 MeV/u  $^{40}\text{Ar}^{18+}$  ions using barrier bucket and stochastic cooling was also realized in ESR [8]. These experimental results demonstrate the principle and feasibility of this stacking method and pave the way for future applications. So far, the stacking scheme utilizing the barrier bucket and beam cooling has been proposed and studied for several heavy ion facilities that are currently under construction, such as FAIR at GSI, NICA at JINR, and HIAF at IMP [9–11].

Generally, the barrier bucket method is based on longitudinal voltage pulses that are synchronized with the ion beam. The barrier voltage is usually created by a broadband rf system consisting of ferromagnetic loaded cavities, and the bandwidth is in the range of tens of kHz to hundreds of MHz. Since 2019, a series of pulsed electron beam cooling experiments have been carried out at HIRFL-CSRm in collaboration with Institute of Modern Physics (IMP) and Jefferson Lab (JLab) [12–14]. For the first time, longitudinal bunching of the coasting ion beam is observed in the experiment. It shows that the ions are captured into a longitudinal space corresponding to the length of the electron pulse, which is due to the barrier voltage created by the space charge field at the electron beam edges. Accordingly, it gives us the idea of accumulating ion beam using only pulsed electron beam in storage rings.

In this paper, we propose this new longitudinal ion beam stacking scheme using a pulsed electron beam, in which beam cooling and barrier bucket can be realized simultaneously. Due to the limitation of the barrier voltage amplitude and the space charge effect in the stacked beam, this method is more suitable for low-intensity beam stacking, such as the accumulation of relatively stable RIBs. The paper is organized as follows: In Sec. II, an overview of the experimental setup and the realization of

\*Corresponding author.  
maolijun@impcas.ac.cn

Published by the American Physical Society under the terms of the *Creative Commons Attribution 4.0 International license*. Further distribution of this work must maintain attribution to the author(s) and the published article's title, journal citation, and DOI.

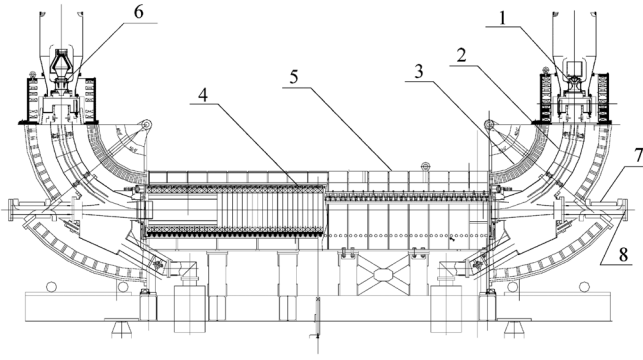


FIG. 1. General layout of the e-cooler EC35 in HIRFL-CSRm. 1-electron gun, 2-electrostatic bending plates, 3-toroid, 4-solenoid of the cooling section, 5-magnet system, 6-collector for e-beam, 7-dipole corrector, 8-flange for CSRm.

the pulsed electron beam are given. In Sec. III, the principle of a barrier bucket created by a pulsed electron beam is introduced, and the stacking scheme and the basic theory of beam dynamics are described. In Sec. IV, simulation results of the beam stacking process in SRing of the HIAF project are presented. In Sec. V, we discuss the optimization and limitation of this stacking scheme. Then, geometric factors of several electron beam distributions are calculated and compared in Sec. VI. Finally a summary is given in Sec. VII.

## II. E-COOLER AND PULSED ELECTRON BEAM GENERATION

Electron cooling is a powerful method to shrink the velocity spread of hadron beams in storage rings on the basis of the Coulomb interaction between a “cold” electron beam and a hadron beam moving at the same average velocity. In the past decades, it has been widely used for beam accumulation and high-precision experiments in several facilities. Up to now, almost all electron coolers built around the world are based on dc electron beams that are accelerated by an electrostatic field. Due to the limitation of the high voltage and the beam power, it is challenging to build a higher-energy dc electron cooler. In order to demonstrate the feasibility of cooling high-energy ion beams using a bunched electron beam, a set of pulsed electron beam cooling experiments has been carried out at HIRFL-CSRm with the collaboration of IMP and JLab. Based on the modified e-cooler EC35 in HIRFL-CSR, cooling with an electron bunch is experimentally demonstrated for the first time [14].

The general layout of the cooler EC35 in CSRm is shown in Fig. 1. The dc electron beam is generated from the thermionic cathode gun, which is located in a high voltage (HV) platform for beam acceleration. The maximum energy of this cooler is 35 keV. Using the toroids and electrostatic bending plates, the electron beam is first delivered to the cooling section and then to the collector for charge recovery. The magnetic system with a longitudinal field is applied

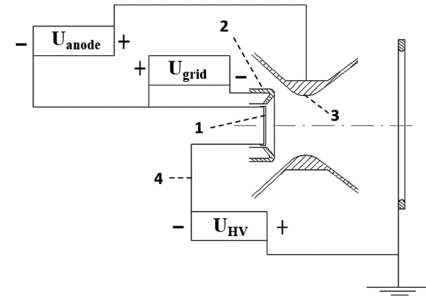


FIG. 2. Schematic view of the EC35 gun. 1-cathode, 2-grid, 3-anode, 4-HV.

along the beam trajectory to control beam size and angular spread and to provide magnetized cooling [15]. Especially, the electron gun is designed with a unique feature. As shown in Fig. 2, a grid electrode located between the cathode and the anode is used to produce a positive/negative electric field at the edge of the cathode, thereby yielding/suppressing the emission of electrons, and generating electron bunches. By changing the ratio of grid to anode potentials, an electron beam with parabolic, flat, or hollow profile in the transverse direction can also be obtained [16].

In the experiments, a solid-state switch driven by a pulse generator is used to rapidly switch the voltage on the grid to generate rectangular electron pulses and leave other properties of the cooler essentially unmodified. The trigger signal is synchronized with the revolution frequency or the rf system to ensure a stable overlap between the electron and ion beams. The time delay and pulse width can be adjusted manually. Figure 3 gives an example of the measured pulsed electron beam with a repetition frequency of 250 kHz and pulse width of 2  $\mu$ s. The BPM signal clearly shows a pulsed electron beam with rectangular distribution, and the measured rise/fall time of the beam current is about 10 ns. With this pulsed electron beam, the cooling of coasting and bunched ion beams is demonstrated for the first time, and the bunching effect on the coasting

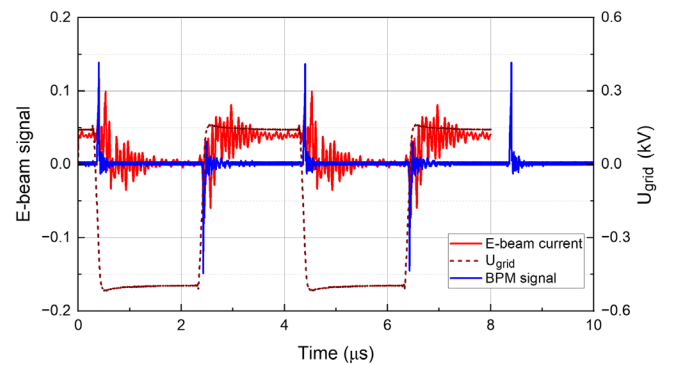


FIG. 3. Modulated voltage on the grid electrode (dash), pulsed electron beam current (red), and BPM signal (blue) generated by the pulsed electron beam in the experiment. The noise of the current signal comes from the filter.

ion beam is also observed. More details and measurements can be found in Refs. [12–14].

### III. BARRIER BUCKET THEORY IN PULSED ELECTRON BEAM COOLING

The basic idea of the longitudinal stacking with a pulsed electron beam is shown in Fig. 4. We assume that the pulsed electron beam has a rectangular distribution in the longitudinal direction, and the beam current varies linearly at the edge. Due to the space charge effect, a longitudinal electric field is generated at the rising and falling edges, thereby generating a barrier voltage. Unlike the fixed barrier bucket stacking scheme, the stable and unstable areas here are separated by the electron pulse itself. Due to the drift motion in phase space, all ion particles will encounter the electron beam and can be cooled to a small momentum spread. With proper settings of bucket voltage and cooling parameters, the ion beam will be eventually trapped in the stable area as long as it coincides with the cooling region. Thereafter, the unstable area is vacated for new beam injection.

As a good approximation for estimating cooling and bunching effects, a round electron beam with uniform distribution in the transverse direction is assumed. Furthermore, we assume the electron pulse repetition frequency is always synchronized with the ion beam. The longitudinal electric field due to space charge can be written as [17]:

$$E_z(\varphi) = -\frac{1}{\beta\gamma^2} \frac{1}{4\pi\epsilon_0 c} \left[ 2 \ln\left(\frac{b}{R_e}\right) + 1 \right] \frac{\partial I_e(\varphi)}{\partial \varphi}, \quad (1)$$

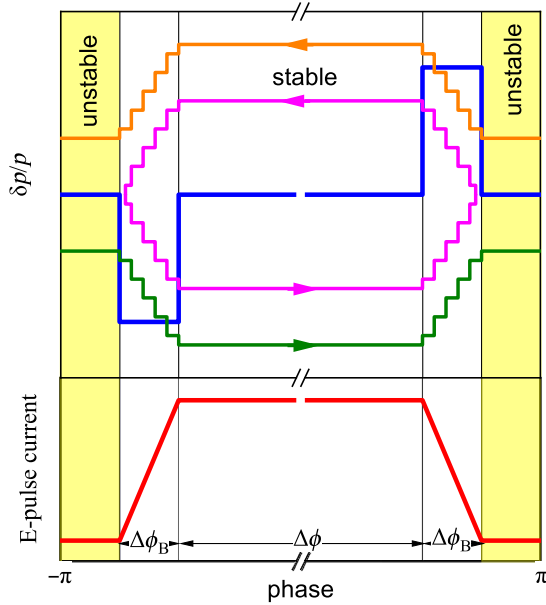


FIG. 4. Schematic view of the barrier bucket generated by a pulsed electron beam, and the particle motion in longitudinal phase space. (Blue: barrier potential in arb. units; magenta: separatrix orbit; orange and green: drift orbit outside the separatrix).

here  $E_z$  is the longitudinal electric field in the laboratory reference frame,  $I_e(\varphi)$  is the electron beam current,  $R_e$  and  $b$  are the radius of the electron beam and the vacuum pipe,  $\epsilon_0$  is the vacuum permittivity,  $\beta$  and  $\gamma$  are the Lorentz factors. For simplicity, we assume a square wave voltage is applied on the grid electrode to generate electron pulses, and the electron beam current increases (or decreases) linearly at the edge. It means the electric field only exists in the rising and falling regions with the length of  $\Delta\phi_B$ . So we have

$$\frac{\partial I_e(\varphi)}{\partial \varphi} = k = \pm \frac{I_e}{\Delta\phi_B}, \quad (2)$$

with  $k > 0$  at the rising edge and  $k < 0$  at the falling edge, respectively. Ions at the edges of the electron pulse will get accelerated (or decelerated) as passing through the cooling section. Compared to the barrier bucket system with rectangular rf wave, the barrier pulse gap here is equal to the electron pulse width  $\Delta\phi$ , the width of the voltage is equal to the rising/falling edge  $\Delta\phi_B$ , and the amplitude of the barrier voltage is determined by the electric field  $E_z$  and the length of the cooler  $L_{\text{cooler}}$ :

$$V_{BB} = |E_z| \times L_{\text{cooler}}. \quad (3)$$

In addition, due to the cooling and bunching effects on the ion beam, the ion space charge needs to be considered. We think the bunched ion beam has the same structure as the pulsed electron beam, so the longitudinal space charge of the ion beam can be described by

$$V_{SC} = \frac{C}{\beta\gamma^2} \frac{1}{4\pi\epsilon_0 c} \left[ 2 \ln\left(\frac{b}{R_i}\right) + 1 \right] \frac{I_i}{\Delta\phi_B}, \quad (4)$$

where  $C$  is the ring circumference and  $R_i$  is the ion beam radius. Naturally, this voltage only exists in the rising and falling regions, and it will gradually cancel the barrier voltage of the pulsed electron beam due to the cooling and beam intensity accumulation. Therefore, a dynamic barrier voltage should be considered during the cooling and stacking process.

To describe the beam dynamics, synchrotron motion, cooling, and intrabeam scattering (IBS) effects of ions need to be included simultaneously. Here we do not expect this method to apply to very high beam intensity, so the transverse space charge and instabilities of the ion beam are not included. We start by considering a single particle with an energy offset  $\Delta E$  relative to the synchronous ion, the particle motion in longitudinal phase space is given by

$$\begin{aligned} \frac{d\varphi}{dt} &= \eta \frac{2\pi}{T_0} \frac{1}{\beta^2} \frac{\Delta E}{E_0} \\ \frac{d\Delta E}{dt} &= \frac{ZeV(\varphi)}{T_0} + [\lambda_{\text{IBS}} - \lambda_{\text{cool}}(\varphi)]\Delta E, \end{aligned} \quad (5)$$

where  $E_0$  is the synchronous energy,  $T_0$  is the revolution period,  $\eta = 1/\gamma_{tr}^2 - 1/\gamma^2$  is the phase slip factor,  $Z$  is the ion charge state,  $\lambda_{IBS}$  and  $\lambda_{cool}$  are the IBS and cooling rates, respectively.  $V(\varphi)$  is the dynamic barrier voltage, which in our case can be written as a piecewise function

$$V(\varphi) = \begin{cases} 0, & -\pi < \varphi \leq -(\Delta\phi_B + \frac{1}{2}\Delta\phi) \\ -V_{BB} + V_{SC}, & -(\Delta\phi_B + \frac{1}{2}\Delta\phi) < \varphi \leq -\frac{1}{2}\Delta\phi \\ 0, & -\frac{1}{2}\Delta\phi < \varphi \leq \frac{1}{2}\Delta\phi \\ V_{BB} - V_{SC}, & \frac{1}{2}\Delta\phi < \varphi \leq (\Delta\phi_B + \frac{1}{2}\Delta\phi) \\ 0, & (\Delta\phi_B + \frac{1}{2}\Delta\phi) < \varphi \leq \pi \end{cases} \quad (6)$$

It shows that the barrier voltage affects only a small fraction of ions in each turn, since usually  $\Delta\phi_B \ll \Delta\phi$ . Therefore, beam dynamics is mainly determined by cooling and IBS effects. Furthermore, electron cooling occurs only in the region where the electron and ion beams overlap. Considering the Parkhomchuk cooling force [18] and the Piwinski IBS model [19], the cooling and IBS rates in the laboratory frame can be simply described as

$$\lambda_{cool}(\varphi) = \frac{4r_e r_n Z^2 \eta_c \ln \xi}{A \gamma^2 \beta [\beta^2 \gamma^2 \frac{\epsilon_{xy}}{\beta_{\perp}} + (\frac{\Delta E}{\beta E_0})^2 + \frac{2T_{eff}}{m_e c^2}]^{\frac{3}{2}}} \frac{I_e(\varphi)}{\pi a^2 e}$$

$$\lambda_{IBS} = \frac{r_n^2 Z^4 c N}{32 \pi^{3/2} A^2 \beta^3 \gamma^4 L_b \sigma_p \epsilon_x \epsilon_y} \langle f(a_i, b_i, c_i) \rangle, \quad (7)$$

where  $r_n$  and  $r_e$  are the classical radii of nucleon and electron, respectively,  $\eta_c$  is the ratio of the cooler length to the ring circumference,  $\ln \xi$  is the coulomb logarithm,  $\beta_{\perp}$  is the beta function at the cooling section,  $T_{eff}$  is the effective energy spread of electron beam,  $c$  is the speed of light,  $\epsilon_x$  and  $\epsilon_y$  are unnormalized emittances,  $L_b$  is the beam length with uniform distribution in longitudinal,  $\langle \rangle$  means averaging of the scattering function  $f$  over the ring with  $a_i, b_i, c_i$  being the beam parameters along the ring ( $i = x, y, p$ ). Here we ignore the dispersion function of the ring. The equations above for beam dynamics calculation are good for simulation but difficult analytically.

Ignoring the space charge effect of the ions, the barrier bucket height generated by the pulsed electron beam can be calculated by

$$\left(\frac{\delta p}{p}\right)_B = \sqrt{\frac{ZeV_{BB}\Delta\phi_B}{\pi\eta\beta^2\gamma A m_0 c^2}} = \sqrt{\frac{ZegI_e L_{cooler}}{2\pi\epsilon_0 A |\eta| \beta^3 \gamma^3 C m_0 c^3}} \quad (8)$$

where  $g = 2 \ln(b/R_e) + 1$  is the geometric factor. In this stacking scheme, particles with momentum spread less than the bucket height will be trapped in the stable region, and its synchrotron oscillation period is given by

$$T_s = T_0 \frac{1}{\eta} \left(\frac{\delta p}{p_0}\right)^{-1} \frac{\Delta\phi}{\pi} + 4T_0 \frac{A\gamma\beta^2 m_0 c^2}{ZeV_B} \frac{\delta p}{p_0}. \quad (9)$$

Due to the cooling and bunching effects, beam stacking can be realized in the stable region and the unstable region is free for new injection. However, this method requires that the stable area coincides with the cooling region, which means it only works for heavy ion beams below transition energy ( $\eta < 0$ ) or negatively charged high energy beams such as antiprotons above the transition energy. Furthermore, since the bucket height is practically limited by the electron beam parameters and the ion longitudinal space charge, this stacking method is not suitable for high-intensity beams with strong space charge or other instabilities.

#### IV. COOLING AND STACKING SIMULATION

The High Intensity heavy-ion Accelerator Facility (HIAF) in China is designed to provide high-intensity and high-energy beams, especially of neutron-rich nuclei far away from the beta stability, for the research of nuclear structure, nuclear astrophysics, atomic physics, etc [11]. As a multifunctional experimental storage ring, the Spectrometer Ring (SRing) of HIAF is designed with several optical operating modes and is equipped with various subsystems such as electron and stochastic cooling, gas-jet target, Schottky resonator, TOF, etc. To accumulate and continuously store secondary or highly charged stable Radioactive Ion Beam (RIBs), for nuclear and atomic physics experiments, an efficient beam stacking method is needed in SRing. As described in Sec. III, the method using a pulsed electron beam could be a solution for this without the need for barrier bucket system.

Based on the design report of the HIAF project, an example of the beam stacking process in SRing using a pulsed electron beam is simulated. In the simulation, we use the multiparticle tracking code TRACKIT [20] and mainly consider magnetized cooling, IBS, electron, and ion longitudinal space charge effects. These modules have already been well developed and benchmarked with the experiments at HIRFL-CSR and RHIC, respectively [21,22]. The main parameters in the simulation are listed in Table I. Here we use the fully stripped stable  $^{238}\text{U}^{92+}$  beam at the energy of 800 MeV/u, which corresponds to the maximum magnetic rigidity of the SRing. The injection beam intensity is  $N_{inj} = 1 \times 10^9$ , which is low enough that the initial space charge effect of the ion beam can be ignored. The electron beam current of 1.0 A is used, which is below the maximum design value of the cooler [23]. Since the bucket height depends on electron beam current, there is no specific requirement for the rising/falling time which is still assumed to be 10 ns. Considering a uniform distribution of electron beam and linearly increased line density, a rectangular barrier voltage of 120.2 V is obtained and applied in the simulation.

TABLE I. Beam parameters in the simulation.

Ring	
Circumference (m)	266.5
Transition energy $\gamma_t$	3.55
$Q_x/Q_y$	4.34/3.64
Average $\beta$ function (m)	9.68/11.65
$\beta_x/\beta_y$ in cooling section (m)	25/25
Cooler length (m)	7.0
Ion beam	
Species	$^{238}\text{U}^{92+}$
Energy (MeV/u)	800
Number of particles per injection	$1 \times 10^9$
rms emittance (x/y) ( $\mu\text{m}$ )	2.0/1.0
rms momentum spread	$4.0 \times 10^{-4}$
Injected beam length ( $\mu\text{s}$ )	0.25
Revolution time ( $\mu\text{s}$ )	1.054
Electron beam	
Current (A)	1.0
Radius (cm)	2.0
Pulse length ( $\mu\text{s}$ )	0.7
Rising/falling time (ns)	10.0
$V_{BB}$ (Volt)	120.2
Bucket height	$0.5 \times 10^{-4}$
Transverse temperature (eV)	0.5
Longitudinal temperature (eV)	$1.2 \times 10^{-3}$
Magnetic field (Gs)	1500
Magnetic field straightness	$5.0 \times 10^{-5}$

Correspondingly, the bucket height is  $0.5 \times 10^{-4}$  according to Eq. (8).

The beam distribution in longitudinal phase space during the cooling process for a single injection is shown in Fig. 5. The electron pulse length is about 70% of the ring circumference. As described in Sec. III, the stacking (stable) and injection (unstable) areas are separated by the electron pulse. Initially, the ion beam with a short bunch length is injected into the unstable area. Subsequently, the ions travel through the cooling section during the drift motion (debunching) and the momentum spread of ions is gradually reduced. When the momentum spread is below the bucket height, ions can no longer escape from the stable area. Finally, most of the ions are cooled and bunched into the stable area, and the unstable area is vacated for the next fresh injection, as shown in Fig. 5. In the simulation, particles with large momentum spread cannot be bunched into the stable region in time, and some of them will be lost at the next new injection.

We know that the equilibrium momentum spread is the result of cooling and IBS effects. A high ion intensity will result in a large beam momentum spread, which is one of the main limitations of the beam stacking performance. Another important limitation is the space charge effect of the ion beam, a high charge intensity can seriously affect the dynamic barrier voltage and even cancel out the stable region.

The beam stacking process is simulated with an injection cycle of 1.0 s. For each new injection, the stored ions located in the unstable region will get lost due to the fast kick. By a combination of single-turn injection and cooling, the number of ions in the ring can be increased several

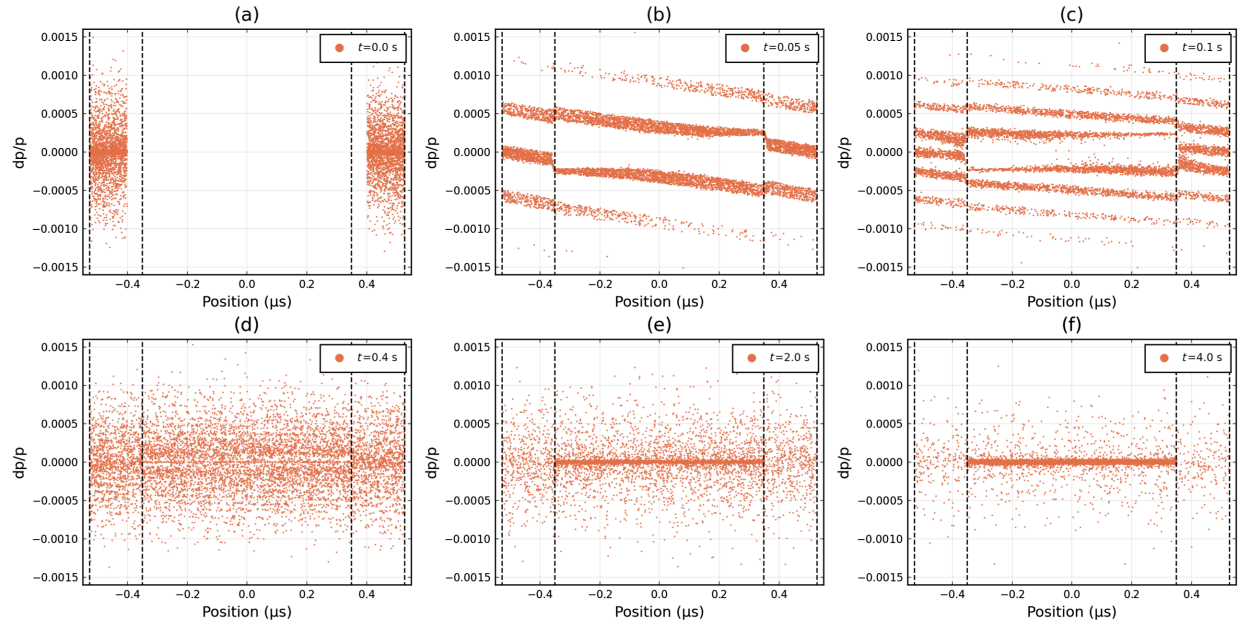


FIG. 5. Simulation results of beam distribution in longitudinal phase space during cooling. The boundaries of the ring and the pulsed electron beam are marked with a dashed line. (a) After injection of a short bunched ion beam (uniform); (b–c) The debunching process due to drift motion, no obvious cooling effect is observed yet; (d) Debunching finished and particles start to be bunched into the bucket due to cooling; (e, f) Ion beam is gradually cooled and bunched into the bucket.

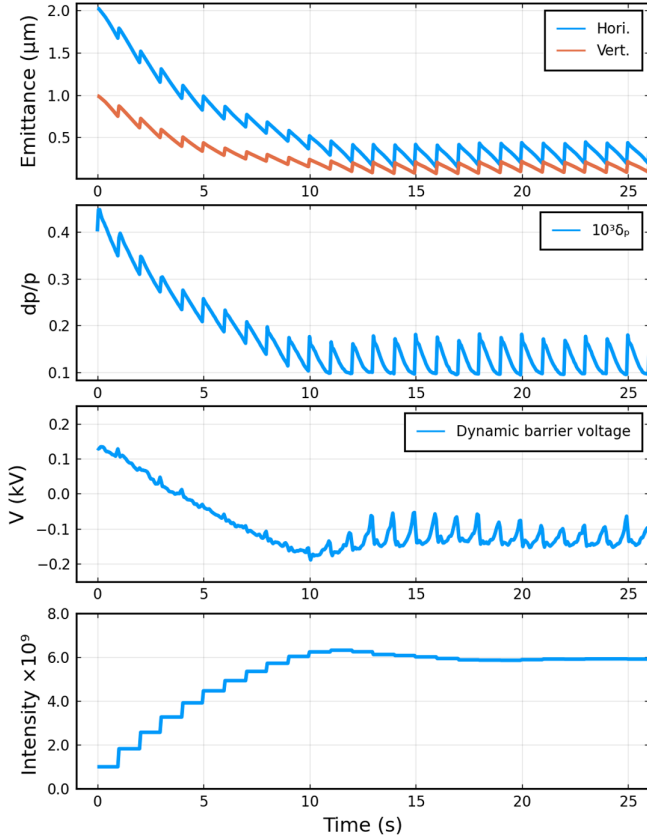


FIG. 6. Evolution of beam emittance and intensity during stacking with an injection interval of 1.0 s.

times. The evolution of beam emittance, momentum spread, dynamic barrier voltage, and beam intensity during stacking is shown in Fig. 6, in which the beam lifetime is not included. We see that the injected beam is cooled rapidly after each injection and accumulated in the ring. However, the stacking efficiency gradually decreases during the stacking process, which is mainly caused by the

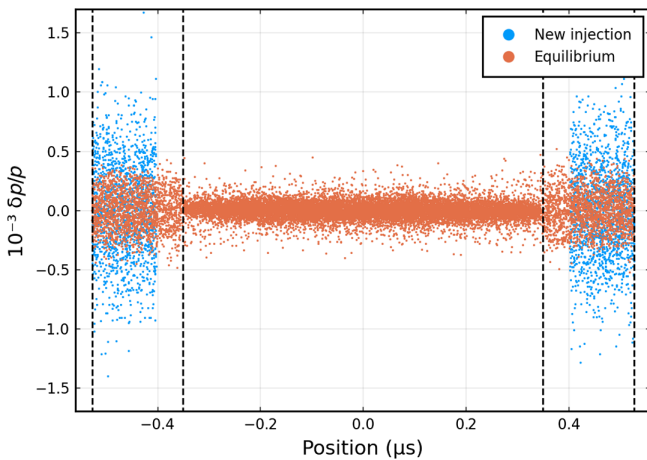


FIG. 7. Particle distribution in longitudinal phase space at equilibrium compared to the injected beam distribution.

reduction of the dynamic barrier voltage during cooling. A negative barrier voltage makes the stable region disappear, and particles at the edge will be kicked out. Finally, an equilibrium state is achieved when the number of lost particles is equal to the injected amount, and the accumulation factor in this case is about 6. The final beam distribution in longitudinal phase space is shown in Fig. 7.

## V. OPTIMIZATION AND LIMITATION

The beam stacking method using a pulsed electron beam is the same as the scheme using a fixed barrier bucket system combined with beam cooling. In both methods, the barrier bucket height is the key factor affecting the stacking performance as well as the cooling process. On one hand, the bucket height should be large enough to capture as many particles as possible into the stable region. On the other hand, a high barrier voltage will induce a large amplitude of ion momentum spread, which makes it difficult for the ions to be cooled in a short period and may be lost at the aperture. Considering ion space charge, the dynamic bucket height makes the stacking process more complicated. Moreover, injection cycle, IBS, and cooling effects can also affect stacking performance. Therefore, all parameters need to be carefully tuned to optimize the stacking process.

As shown in Fig. 8, a comparison of the stacking process of 800 MeV/u  $^{238}\text{U}^{92+}$  in SRing under different parameters is presented. It is clear that a small electron beam size or high current can improve the stacking performance because the cooling rate as well as the bucket height are proportional to the electron density. Besides, it shows that stacking occurs even without the electron beam, which is caused by the effect of longitudinal painting that is contributed by the drift motion in phase space. When a pulsed electron beam is applied, the stacking performance is increased, and the efficiency depends on the injection cycle. The small difference in the maximum density in Fig. 8 is due to the difference in the equilibrium state under different parameters.

We know that the barrier voltage only affects a small fraction of ions, so the equilibrium state is mainly determined by the cooling and IBS effects. In order to verify the effectiveness of this stacking method for different beams at different energies, we simply assume that the velocity distributions of both electron and ion beams are isotropic. Based on Eq. (7), the dependence of the cooling and IBS rates on beam parameters can be simplified to

$$\lambda_{\text{cool}} \propto -\frac{Z^2 n_e}{A\gamma^2}$$

$$\lambda_{\text{IBS}} \propto \frac{Z^4 N}{A^2 \beta \gamma^2 \delta p/p}. \quad (10)$$

where  $n_e$  is the local density of the electron beam,  $N$  is the particle number, and  $\delta p/p$  is the rms momentum spread.

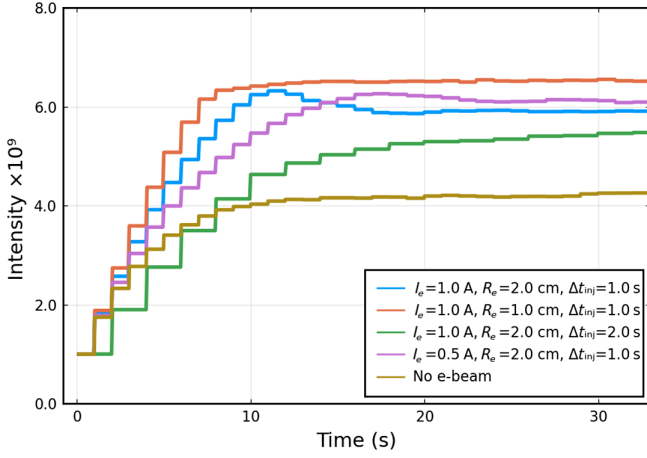


FIG. 8. Comparison of the stacking process with different settings in simulation.

The equilibrium is achieved when  $\lambda_{\text{cool}} + \lambda_{\text{IBS}} = 0$ . Here we assume the maximum intensity of the stored beam is reached when the equilibrium momentum spread is equal to the bucket height. Then, the dependence of the final stored particle number on beam parameters can be estimated based on Eqs. (8) and (10),

$$N \propto \sqrt{\frac{gAn_e^3 a^2}{|\eta|Z^3 \gamma^3}}. \quad (11)$$

It shows that the energy, charge state of ion, and electron beam density are the main parameters that affect the stacking performance. In addition, the geometric factor  $g$  of the electron beam also has an effect on the accumulation efficiency, which will be discussed in Sec. VI. Using the  $^{238}\text{U}^{92+}$  beam as a reference, the maximum stacking intensities for several ion species are estimated, as listed in Table II. It shows that this stacking method is suitable for almost all ion species in SRing, especially for the ions with a small mass-to-charge ratio and medium energy.

In HIAF, the primary goal of SRing is to accumulate secondary or stripped ion beams (RIBs) for various experiments, typically at medium energy and low intensity.

TABLE II. Estimation of stacking result on other ions.

Ion	Z	A	$E_0$ (MeV/u)	$\sqrt{Z^3/A}$	Estimated $N_{\text{stacking}}$
U	92	238	800	57.2	1.00
Sn	50	132	740	30.8	1.87
Sn	50	104	740	34.7	1.66
Xe	54	131	900	34.7	1.64
Kr	36	84	950	23.6	2.41
Kr	36	84	600	23.6	2.48
Ar	18	40	1000	12.1	4.71
C	6	12	600	4.2	13.8
C	6	12	1500	4.2	14.3

Electron cooling has been demonstrated to be extremely successful in cooling medium energy ions. Based on the cooler design and simulation results in SRing, we conclude that the beam stacking method using a pulsed electron beam could be a candidate for the beam stacking scheme.

## VI. GEOMETRIC FACTOR

In the above, a uniform transverse distribution of the electron beam is considered, which is not always true. Sometimes, a Gaussian distribution or hollow electron beam is needed to optimize the cooling process, which has a strong effect on the longitudinal and transverse space charge impedance. Since the barrier voltage is mainly caused by the longitudinal space charge field of the electron beam, it is necessary to compare the differences between different electron beam distributions.

Assuming a round electron beam, the local beam density can be described by  $\rho(r, s) = f(r)\lambda(s)$  with  $f(r)$  the transverse distribution and  $\lambda(s)$  the linear density in the longitudinal direction. The function  $f(r)$  should satisfy the condition:

$$\int_0^{R_e} 2\pi r \rho(r) dr = 1, \quad (12)$$

where  $R_e$  is the radius of the electron beam. For a perfectly conducting beam pipe, the longitudinal space charge field can be calculated by

$$E(s) = \frac{eg}{4\pi\epsilon_0\gamma^2} \frac{\partial\lambda(s)}{\partial s}, \quad (13)$$

where the geometric factor is [24]

$$g = \int_0^b \frac{2}{x} \int_0^x 2\pi r f(r) dr dx, \quad (14)$$

where  $b$  is the pipe radius. Actually, the geometric factor is dependent on the radial position. In our case, since the ion beam size is quite small after cooling, we only consider the electric field on axis. This factor for beams with various distributions has been modeled in Ref. [24]. Here, we mainly study this factor for hollow electron beam. Based on the experimental measurement of the hollow electron beam in Ref. [16], we simply assume that the hollow beam is a Gaussian distribution with a position offset  $r_0$  (hollow radius) and small variance  $\sigma_r$ :

$$f(r) = \frac{A_N}{2\pi\sigma_r^2} \exp\left[-\frac{(r-r_0)^2}{2\sigma_r^2}\right], \quad (15)$$

with

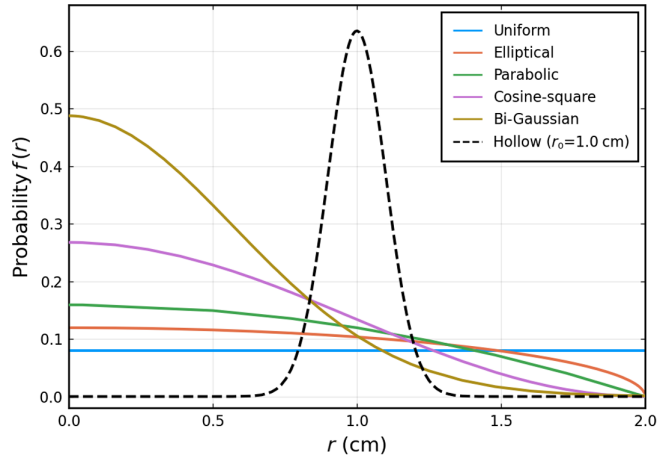


FIG. 9. Various beam transverse distribution  $f(r)$  with beam radius  $R_e = 2$  cm.

$$A_N = \frac{\sigma_r}{r_0 \sqrt{\pi/2} [1 + \operatorname{erf}(\frac{r_0}{\sqrt{2}\sigma_r})] + \sigma_r \exp(-\frac{r_0^2}{2\sigma_r^2})}. \quad (16)$$

For example, Fig. 9 presents several transverse distributions with the beam radius  $R_e = 2$  cm, where  $r_0 = 1.0$  cm and  $\sigma_r = 0.1$  cm for hollow electron beam.

With the pipe radius  $b = 10$  cm, the numerical integrals for various beam distributions are calculated using Eq. (14), and the dependence of the geometric factor on electron beam radius is presented, as shown in Fig 10. For the hollow distribution, the hollow radius is set as  $r_0 = 0.5$  cm and  $r_0 = 1.0$  cm, respectively, and the variance is set to  $\sigma_r = R_e/20$ , which determines the beam density. It shows that the  $g$  factor strongly depends on the electron beam radius. Usually, the radius of the electron beam in the cooler is between 1.0 and 2.0 cm, we think there are no clear differences for different beam distributions. Hollow electron beam can also be applied to the application of ion stacking.

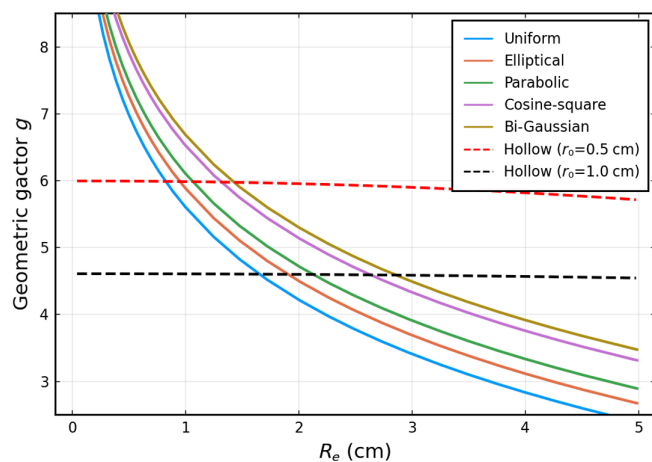


FIG. 10. Dependence of the geometric factor on beam radius for various electron beam distributions.

## VII. SUMMARY

Experiments show that the space charge field of the electron pulse can provide a barrier bucket in storage rings, which can be implemented on longitudinal beam stacking. The simulation shows the possibility of ion beam stacking using the pulsed electron cooling method. The influence of electron beam parameters on the stacking process is analyzed numerically. We expect such a simple way can be applied on the beam stacking in medium energy heavy ion storage rings, such as SRing in HIAF.

## ACKNOWLEDGMENTS

The authors would like to thank T. Katayama for useful suggestions and discussions. This work is supported by the Chinese Academy of Sciences (No. E229521Y), the National Key R&D Program of China (No. 2019YFA0405400), and the National Natural Science Foundation of China (No. 12275323, 12275325 and 12205346)

- [1] J. E. Griffin, C. Ankenbrandt, J. A. MacLachlan, and A. Moretti, Isolated bucket rf systems in the Fermilab anti-proton facility, *IEEE Trans. Nucl. Sci.* **30**, 3502 (1983).
- [2] C. M. Bhat, Barrier rf systems in synchrotrons, Fermi National Accelerator Laboratory (FNAL), Batavia, IL, Technical Report No. FERMILAB-Conf-04/091-AD, 2004.
- [3] C. M. Bhat, Applications of barrier bucket RF systems at Fermilab, Fermi National Accelerator Laboratory (FNAL), Batavia, IL, Technical Report No. FERMILAB-CONF-06-102-AD, 2006.
- [4] M. Fujieda, Y. Iwashita, A. Noda, Y. Mori, C. Ohmori, Y. Sato, M. Yoshii, M. Blaskiewicz, J. M. Brennan, T. Roser, K. S. Smith, R. Spitz, and A. Zaltsmann, Barrier bucket experiment at the AGS, *Phys. Rev. ST Accel. Beams* **2**, 122001 (1999).
- [5] T. Bohl, E. Shaposhnikova, and T. P. R. Linnekar, Thick barrier buckets using the SPS travelling wave structures, CERN, Technical Report No. SL-Note-2000-032-HRF, 2000.
- [6] K. Takayama, J. Kishiro, M. Sakuda, Y. Shimosaki, and M. Wake, Superbunch Hadron Colliders, *Phys. Rev. Lett.* **88**, 144801 (2002).
- [7] C. Dimopoulou, B. Franzke, T. Katayama, G. Schreiber, M. Steck, and D. Möhl, Longitudinal accumulation of ion beams in the ESR supported by electron cooling, in *Proceedings of Workshop on Beam Cooling and Related Topics, Montreux, Switzerland* (CERN, Geneva, 2007), p. 21.
- [8] M. Steck, C. Dimopoulou, B. Franzke, O. Gorda, T. Katayama, F. Nolden, G. Schreiber, D. Möhl, R. Stassen, H. S. FZJ *et al.*, Demonstration of longitudinal stacking in the ESR with barrier buckets and stochastic cooling, in *Proceedings of the 2011 IEEE COOL Chips XIV* (IEEE, New York, 2011), Vol. 11, p. 140.

- [9] P. Spiller and G. Franchetti, The FAIR accelerator project at GSI, *Nucl. Instrum. Methods Phys. Res., Sect. A* **561**, 305 (2006).
- [10] G. Trubnikov *et al.*, NICA project at JINR, in *Proceedings of the 4th International Particle Accelerator Conference, IPAC-2013, Shanghai, China, 2013* (JACoW, Shanghai, China2013), TUPFI009.
- [11] J. C. Yang *et al.*, High intensity heavy ion Accelerator Facility (HIAF) in China, *Nucl. Instrum. Methods Phys. Res., Sect. B* **317**, 263 (2013).
- [12] L. J. Mao *et al.*, Experimental demonstration of electron cooling with bunched electron beam, in *Proceedings of 11th International Workshop on Beam Cooling and Related Topics, Bonn, Germany* (JACoW, Geneva, Switzerland, 2018), TUP15.
- [13] H. Zhao, L. Mao, Y. Zhang, H. Wang, J. Yang, T. Powers, M. Tang, J. Li, X. Ma, X. Yang, K. Jordan, S. Wang, H. Zhang, Z. Dong, and M. Spata, Simulation of ion beam cooling with a pulsed electron beam, *Nucl. Instrum. Methods Phys. Res., Sect. A* **902**, 219 (2018).
- [14] M. W. Bruker *et al.*, Demonstration of electron cooling using a pulsed beam from an electrostatic electron cooler, *Phys. Rev. Accel. Beams* **24**, 012801 (2021).
- [15] Y. S. Derbenev and A. N. Skrinsky, The effect of an accompanying magnetic field on electron cooling, *Part. Accel.* **8**, 235 (1978), <https://cds.cern.ch/record/1107957>.
- [16] A. Buble, A. Goncharov, A. Ivanov, E. Konstantinov, S. Konstantinov, A. Kryuchkov, V. Parkhomchuk, V. Reva, B. Skarbo, B. Smirnov, B. Sukhina, and M. Tiunov, The electron gun with variable beam profile for optimization of electron cooling, in *Proceedings of the 8th European Particle Accelerator Conference, Paris, 2002* (EPS-IGA and CERN, Geneva, 2002).
- [17] A. Hofmann, Single-beam collective phenomena-longitudinal, [10.5170/CERN-1977-013.139](https://cds.cern.ch/record/105170), 1977.
- [18] V. Parkhomchuk, New insights in the theory of electron cooling, *Nucl. Instrum. Methods Phys. Res., Sect. A* **441**, 9 (2000).
- [19] A. Piwinski, Intra-beam scattering, in *Proceedings of 9th International Conference on High-Energy Accelerators, Stanford, CA* (A.E.C., Washington, DC, 1974), pp. 405–409.
- [20] Code available at <https://github.com/hezhao1670/ECool-TRACKIT>.
- [21] H. Zhao, L. Mao, J. Yang, J. Xia, X. Yang, J. Li, M. Tang, G. Shen, X. Ma, B. Wu, G. Wang, S. Ruan, K. Wang, and Z. Dong, Electron cooling of a bunched ion beam in a storage ring, *Phys. Rev. Accel. Beams* **21**, 023501 (2018).
- [22] H. Zhao, M. Blaskiewicz, A. V. Fedotov, W. Fischer, X. Gu, D. Kayran, J. Kewisch, C. Liu, S. Seletskiy, V. Schoefer, and P. Thieberger, Cooling simulation and experimental benchmarking for an rf-based electron cooler, *Phys. Rev. Accel. Beams* **23**, 074201 (2020).
- [23] L. Mao *et al.*, The electron cooling system for the HIAF project in China, in *Proceedings of COOL'19: 12th Workshop on Beam Cooling and Related Topics* (JACoW Publishing, Geneva, Switzerland, 2019), pp. 14–17, [10.18429/JACoW-COOL2019-MOZ01](https://cds.cern.ch/record/1018429).
- [24] K. Y. Ng, Space-charge impedances of beams with non-uniform transverse distributions, Technical Report No. FERMILAB-FN-0756, Fermi National Accelerator Laboratory (FNAL), Batavia, IL, 2004.